

Analysis of energy outputs photovoltaic power plants under extremes climatic conditions - Case of the Sahel

Abstract

The present work analyzes the energy production of three $50kW_p$ photovoltaic (PV) power plants which are placed in three climate zones. The Sudano-Sahelian and Sudanian climates have lower average temperatures than the Sahelian environment. The Sudanian climate, next the Sudano-Sahelian zone, and finally the Sahelian region, have the best performance for PV power plants. The performance of silicon PV cells may suffer due to temperature. The Sahelian climatic zone experiences its highest levels of PV output between April and October due to longer sunshine hours and a reduction in sand dust. In the Sudano-Sahelian region, PV output is at its peak between May and October. The best PV generation in the Sudanian environment occurs between June and November. The theoretical forecasting for the various climate zones is consistent with the PV mini-grid real energy output in various situations. The humidity, cloud cover, and rainfall in all climatic zones will make August the worst month for PV energy generation. Due to the type of load compared to the Sudanian climate where the PV power plant is situated in a university, the usage of batteries is crucial in the Sudano-Sahelian climate.

Keywords: PV power plant, Silicon PV module, Electricity grid, Sahelian climate.

1. Introduction

In many emerging nations, there is a surge in energy demand. Due to climate change, renewable energy sources offer a significant chance to supply electricity to emerging nations reducing greenhouse gas emission. According to Plaza *et al.* and Mohamed *et al.* [1, 2], the PV panels' performance was impacted by the high ambient temperatures, dusty air, and cloud cover. Burkina Faso is a Sahelian developing nation whose national electricity rate rose from 13.7% in 2008 to 21.5% in 2018[3]. This rate of electrification is primarily dominated by urban electrification. The rural electrification has only increased from 1% to 3.2% during the same period. The gap between urban and rural areas is common to all Sahelian nations. It varies just slightly from a country to other. From 21.9% in 2008 to 16.9% in 2018 [3], Burkina Faso's national production of renewable energy has decreased. This decrease is the result of increased conventional energy use to meet the explosion of the energy demand. However, SONABEL, the country's electricity provider, increased the installed PV power plant in Burkina Faso from $30kW_p$ in 2011 to $34.899MW_p$ in 2018 [3]. Private PV production increased from $9.1GWh$ in 2017 to $54.1GWh$ in 2018 [3, 4]. To conserve the environment, it translates to a greater awareness of the need to consume less conventional energy. Accord-

ing to Ouedraogo *et al.*[5], the use of PV energy can increase a population's reliance in regions with high security unrest. Furthermore, a variety of activities utilize solar energy especially in remote areas (figure 1).



Figure 1: Surveillance camera powered by PV energy to control road traffic in the City of Ouagadougou (Burkina Faso)

Mohammed ([2]) asserts that Saharan sand accumulation affects PV module performance. Sahel is an area closeness to the Sahara. But the climatic conditions in the Sahel are different from those in the Sahara. Regarding the functionality of PV systems under Sahelian climate conditions, there is a dearth of deep knowledge. It is then very instructive to examine the PV power plant energy production in Sahel climate condition in order to recognize where the greatest losses occur and can reduce the overall efficiency. The Sahelian nation of Burkina Faso in West Africa was chosen to perform research on the PV system's capacity to create electricity in order to fill this deficit. The Sahelian strip's energy production can be estimated using information on Burkina Faso's PV energy output due to its geographic location. The usage of PV energy is widespread in Burkina Faso to meet the country's high energy demand. In hospitals and other public institutions around Burkina Faso in various climate zones, PV systems have been deployed during the past two years. Three climate areas are shown in Burkina Faso in figure 2.



Figure 3: PV system in roofing of shop in Ouagadougou City

According to certain research ([8, 9, 10, 11]), a strong electromagnetic field might disturb a PV cell energy production. Compared to electromagnetic field variation, the thermodynamic and absorption processes exhibit greater sensitivity. The critical junction being crossed by the carriers' charge and resulting increase in short circuit current is the explanation for the electromagnetic sensitivity of the absorption phenomenon. On the other hand, the open-circuit voltage, which falls as the electromagnetic field increases, substantially influences the thermodynamic electromagnetic sensitivity. Then for the PV system, the influence of the electromagnetic source must be control anywhere to avoid the performance reduction. Some areas have a background level of radioactivity that is significantly higher than the average background. There may be some lost ionizing radiation sources around PV installation. The PV cell's performance may suffer as a result of increased carrier charge recombination brought on by low radiation [20]. The high background site is to avoid for a PV system installation. Dust is an important issue to take into account in the Sahelian zone. It can fall onto the PV module's electrical outputs and have an impact on PV systems [5] as presented in the figure 3. The present research intends to assess the theoretical PV energy production and the *in-situ* energy production of the PV system deployed in the various climatic circumstances and make some recommendations to optimize the deployment of the PV energy in the Sahelian countries, using the example of Burkina Faso. The theories and techniques regarding a PV system dimensioning in the various climate zones are discussed in Section 2. The findings and discussions will be presented in Section 3. This section will draw a comparison between theoretical and on-site production. The latter component of the paper will contain some conclusions.

2. Theories and Methods

The present section is about three (03) mini-grids installed in the different climate zones in hospitals and universities. They are the mini-grid installed in university of Ouahigouya in Sahelian climate, the mini-grid installed in the Paediatric Charles De Gaulle of Ouagadougou in the Sudano-Sahelian climate and the last which is installed in Nazi Boni University of Bobo

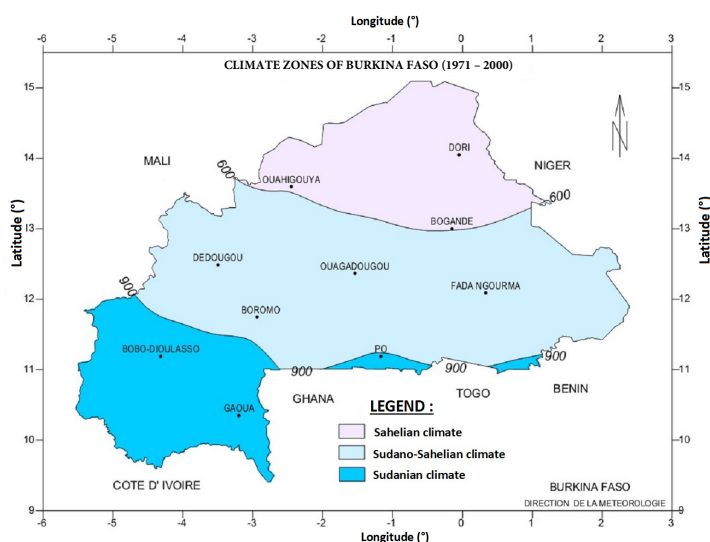


Figure 2: Climate zones of Burkina Faso based on the 1971-2000 average annual rainfall

The average temperature in these three zones rises from the west and south (Banfora, Bobo Dioulasso, Gaou and Niangoloko) to the north (Bogande, Dori and Ouahigouya)[6]. Therefore, the West and South may produce more PV energy than the North and East, at least in theory. The North and East's extreme heat is the main contributor. Mali, Niger, Mauritania, and Chad all experience a comparable predicament. According to Ouedraogo [6] and Cotfas [7], a rise in temperature can lead to a reduction in the performance of a PV cell by decreasing the thermodynamic efficiency and the fill factor (FF) during a heat wave. Sometimes the PV system is installed close to the source of the electromagnetic radiation such as base transceiver station (BTS), radio and television (TV) antenna [8].

Dioulasso in the Sudanian climate. Each one PV power plant has a peak power of $50kW_p$. The theoretical background about sizing up and the informations about selected equipments will be provided. The technical specifications about grid synchronization and natural phenomena which can cause damages will be provided also at the end of this section.

2.1. Theoretical background

The theoretical daily energy production for PV module area $A_{PV}(m^2)$ was defined by [12] as:

$$P_{PV_{rated}} = A_{PV} \cdot G_{av} \cdot \eta_{PV} \quad (1)$$

With $G_{av}(W.m^{-2})$, the average global solar irradiation of the site and η_{PV} is the PV module efficiency in Standard Test Conditions (STC). The peak power occurs for $G_{av} = G_{STC}$. This approximation can be extrapolated on the PV system set when the installed PV system area is known. The output power based on the ambient temperature and the global radiation can be found following [13, 14] as:

$$P_{PV_{out}} = P_{PV_{rated}} \frac{G_{av}}{G_{STC}} [1 + \alpha_T (T_c - T_{STC})] \quad (2)$$

Where $P_{PV_{rated}}$ is the rated power of the utilized PV module. α_T refers to the temperature coefficient (in this case $-3.7 \times 10^{-3} \text{ } ^\circ\text{C}^{-1}$), T_{STC} is the reference temperature (in STC 25°C), and G_{STC} the reference solar radiation (in STC $1000W.m^{-2}$). The PV cell temperature T_c can be formulated as follows [13, 14]

$$T_c = T_{amb} + \left(\frac{NOCT - 20}{800} \right) G_{av} \quad (3)$$

With T_{amb} , the ambient temperature ($^\circ\text{C}$) and $NOCT$, the normal operating cell temperature ($^\circ\text{C}$). The PV modules electrical model is presented on the figure 4 [14].

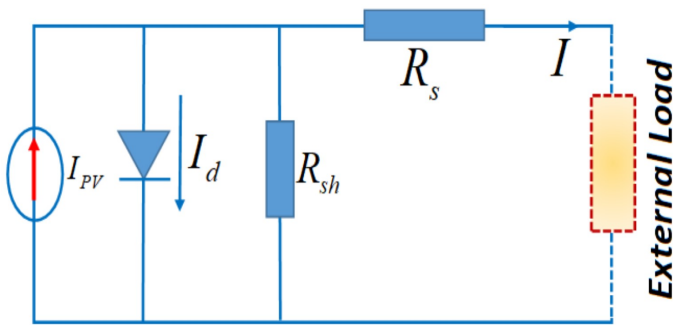


Figure 4: PV module electrical model

The current per PV module versus the voltage that we are going to extrapolate to the system's total current is shown in the following equation [6].

$$I = N_p I_{PV} - N_p I_o \left[\exp \left(\frac{N_s V + R_s I \left(\frac{N_s}{N_p} \right)}{a N_s V_T} \right) - 1 \right] - \frac{N_s V + R_s I \left(\frac{N_s}{N_p} \right)}{R_{sh} \left(\frac{N_s}{N_p} \right)} \quad (4)$$

Whith N_p the number of PV modules in parallel and N_s the number of PV modules connected in series. I_o gives the saturation current caused by the $p-n$ junction, R_s the series resistance, R_{sh} the shunt resistance, V_T provides the thermal voltage and a provides the ideality factor. It is given for different types of silicon PV cells in the table 1.

Table 1: Ideality factor a versus PV cell technology [15]

Technology	a
Mono crystalline silicon (<i>Si - mono</i>)	1.2
Polycrystalline silicon (<i>Si - poly</i>)	1.3
Amorphous hybrid silicon (<i>a - Si : H</i>)	1.8

The photogenerated current versus the solar radiation and the temperature is found as [16]

$$I_{ph} = \frac{G}{G_{STC}} \left[I_{ph_{ref}} + k_T (T_c - T_{STC}) \right] \quad (5)$$

With k_T is the temperature coefficient of the short circuit current ($A.^\circ\text{C}^{-1}$). The saturation current I_o is evaluated according to the next formula [16].

$$I_o = I_{o_{ref}} \left(\frac{T}{T_{STC}} \right)^3 e^{\left[\frac{q E_g}{a k_B} \left(\frac{1}{T_{STC}} - \frac{1}{T} \right) \right]} \quad (6)$$

Where $I_{o_{ref}}$ is the saturation current in the STC, q is electron charge, k_B is Boltzmann's constant and E_g is the band-gap energy in electron-volt (eV).

The second component of the PV system is the battery storage bank. At an output power of the PV system higher than the required load, the energy storage unit will start charging. The energy storage is used during the insufficiency of the output to supply the load demand. When charging, the state of the battery storage at time t , $S_{bat}(t)$ is formulated following [12, 14]

$$S_{bat}(t) = (1 - \sigma) S_{bat}(t-1) + \left(E_{PV}(t) - \frac{E_L(t)}{\eta_{inv}} \right) \eta_b \quad (7)$$

Where $E_L(t)$ is the load energy demand at time t , η_{inv} is the efficiency of the inverter, η_b the battery storage efficiency and σ the self-discharge rate.

To supply the deficit, the battery storage is discharged according to the following expression [12, 14]:

$$S_{bat}(t) = (1 - \sigma) S_{bat}(t-1) + \left(E_{PV}(t) - \frac{E_L(t)}{\eta_{inv}} \right) \eta_{bd}^{-1} \quad (8)$$

With η_{bd} the battery discharging efficiency.

2.2. Sizing of the PV system

To meet the load demand, it is necessary to evaluate the energy consumption profile of the load (e.g., Hospitals, University, etc.). From this load profile, the profile of the daily energy demand ($C_d(Wh)$) is obtained using the following formula [12, 17]:

$$C_d = P_L \cdot t \quad (9)$$

Where $t(h)$ is the load operation duration and $P_L(W)$ the load power. The peak power of the photovoltaic field to be installed

is deducted from the month-of-the-year with the worst solar incidence using the expression [17]:

$$P_c = \frac{C_j}{K.E} \quad (10)$$

$E(kWh/m^2/day)$ is the solar incident energy on the plan of the PV modules. Its value is between $3kWh.m^{-2}.day^{-1}$ and $7.5kWh.m^{-2}.day^{-1}$ in Burkina Faso for different climate zones[18]. K is the correction factor taking into account the different efficiencies and the security coefficients. It is generally choosing between 0.55 and 0.65. Its practical value is $K = 0.65$.

The number of PV modules required to produce the required amount of solar energy is estimated by [12]:

$$N_{pv} = \frac{P_c}{P_{mp}} \quad (11)$$

P_{mp} is the maximum power of the selected PV module. In Figure 5, it is represented the block diagram.

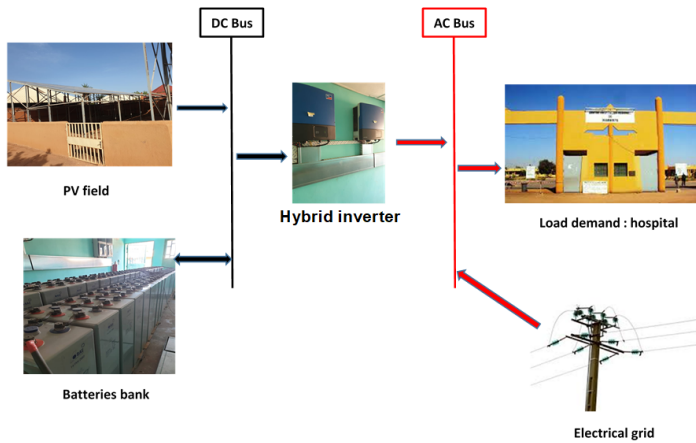


Figure 5: Block diagram of a PV system set [5]

In the present study there is only the input energy from the national grid and not the provided energy from PV plant to national grid. PV plant energy is provided only to the internal load. The national grid is used to inject the PV energy in the local network of the load. Note that the solar energy is withdrawn only in two cases: at night when the batteries are completely discharged and in the absence of PV production. In alternative current (AC), the $C_j(Wh/day)$ is given by

$$C_j = \frac{\sum_i P_i t_i}{\eta_{DC/AC}} \quad (12)$$

Whith $\eta_{DC/AC}$ is the inverter efficiency. The PV field electricity is found in direct current (DC) which will be inverted to an alternative current (AC) for the load use. P_i is the individual equipment power and t_i functioning duration. The output

power of the inverter (P_{inv}) is obtained, according to [14] by the following equation:

$$P_{inv} = \frac{P_d}{\eta_{inv}} \quad (13)$$

With P_d the hourly demand and η_{inv} is the inverter efficiency. The PV modules network is provided by :

⇒ Total number of PV modules [12, 17].

$$n_t = \frac{P_c}{P_{mp}} \quad (14)$$

⊗ The series connection PV modules number is [17] :

$$n_s = \frac{U_{string}}{U_{mp}} \quad (15)$$

U_{string} the string maximum voltage supplied and U_{mp} is the individual module voltage in PV module maximum power point.

⊗ String number [17].

$$n_p = \frac{n_t}{n_s} \quad (16)$$

⇒ Grid inverter DC/AC

The sufficient inverter quantity is given by :

$$n_{inv} = \frac{P_c}{P_{inv}} \quad (17)$$

With P_{inv} , the inverter individual power. The total string by inverter is found as :

$$n_{string/inv} = \frac{n_p}{n_{inv}} \quad (18)$$

⇒ Batteries charging inverter

Active power for the year (365 days) is obtained by

$$P_{act} = \frac{1}{H} \frac{P_c \cdot P_r}{365} \quad (19)$$

P_r provides the productive PV power which is between $1600kWh.kWp^{-1}.year^{-1}$ to $1800kWh.kWp^{-1}.year^{-1}$ in Burkina Faso [18] under H as the daily sunshine duration with a power factor of $\cos(f)$. The charging inverter number is given by

$$n_{char-inv} = \frac{P_{act}}{P_{inv}} \quad (20)$$

⇒ Batteries quantity

The storage capacity requirement of the battery system in Ampere-hour (Ah) can be found as [12, 17]:

$$C(Ah) = \frac{C_d \times A_d}{U_s \times \eta_{bat} \times \eta_{inv} \times DoD} \quad (21)$$

A_d represents the battery autonomous days i.e. the maximum number of days the battery can supply continuous energy without recharging, DoD is the battery maximum depth of discharge permissible and U_s is the system voltage in Volts(V). The string number of the batteries can be evaluated ([12, 17]):

$$n_{String-b} = \frac{C(Ah)}{C_{ind}} \quad (22)$$

C_{ind} provides the individual battery storage capacity i.e. its nominal capacity in Ampere hour (Ah).

⊗ The batteries number in series

$$N_{Series-b} = \frac{U_s}{U_{bat}} \quad (23)$$

Here U_s is the delivered voltage provided by the PV field. For $P_c \geq 1kW_p$, $U_s = 48V$.

⊗ The total number of the batteries is obtained as following

$$N_{T-b} = N_{Series-b} \cdot N_{String-b} \quad (24)$$

The charging and the discharging of the battery bank can follow the equations 7-8. The following table 2 provides some informations about the load. An identical peak power ($50kW_p$)

Table 2: Load sheet

Designation	Energy consumption $C_d(Wh)$
surgical wing	116817
emergency	46 033
Total	162 850

was installed in the three climate zones of Burkina Faso. The hospital is then chosen as reference to the load estimation. In a previous paper [5], the integral estimation was summarized and provided in the table 2.

The energy evaluation is done for 3.5h and the batteries autonomy is 3.5h. The PV module electrical manufacturing specifications is presented in the table 3.

Table 3: Electrical manufacturing specifications of PV module

P_{Max}	$330W_p$
U_{MP}	$38V$
I_{MP}	$8.69A$
U_{oc}	$45.5V$
I_{sc}	$9.2A$

The technical specifications of the batteries are indicated in the table 4. The wire of the various system components can be obtained using a numerical tool. A security sizing of the installation has been incorporated in order to safeguard and secure the PV system. In the system, the surge arrester will be included. A few defense mechanisms will also be added against natural events which can harm PV modules (rain, dew, wind and sun). The PV power plant is operated as :

Table 4: Batteries OPzV data

U_{bat}	$2V$
Capacity C_{10h}	$2000Ah$
Efficiency	95%

- The PV energy will supply in priory the loads during the day;
- During the unavailability of the PV energy, the national electricity company (SONABEL) will provide the energy to the load ;
- The batteries will supply when the SONABEL and the PV power plant are not in operation.

This study is carried out so far any telecommunication antenna and also any high radioactive background for the three PV systems.

3. Results and Discussions

3.1. Theoretical production of PV energy in different climatic zones

The Sahelian climate is found in the north of Burkina Faso (zone 1); the Sudano-Sahelian climate is found in the center, the northwest, the east, and the south of the country (zone 2); and the Sudanian climate is found in the west (zone 3). Images of the three zones' PV installations are displayed in Figure 6.



Figure 6: $50kW_p$ power plant installed in the three climatic zones of Burkina Faso

In the zone 1, the PV system is installed in the University of Ouahigouya, the capital city of the Yenenga province. In the zone 2, the system is installed in the Pediatric Hospital called *Hopital pediatrique Charles De Gaulle* in the capital City Ouagadougou. In the climatic zone 3, the installation is done in the premises of the Nazi Boni University of Bobo Dioulasso. The solar radiation and the temperature data used to evaluate the theoretical PV energy production are found from the national meteorology services (ANAM). Figure 7 shows the interannual

variations of the average temperature from 2010 to 2016 for three cities in the three climate zones.

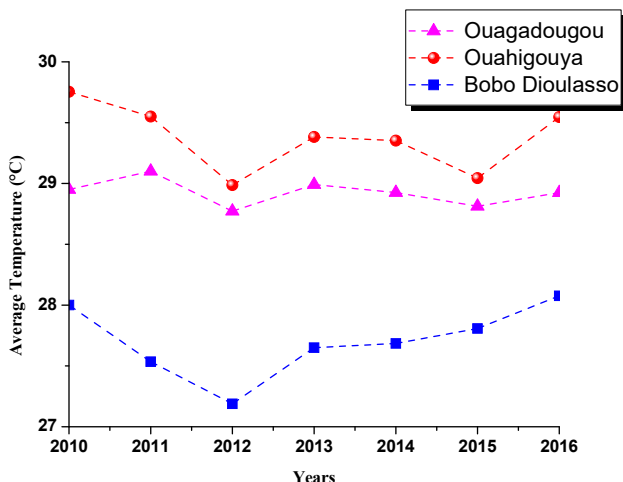


Figure 7: Interannual variability of the average air temperature in three different climatic zones of Burkina Faso

This graph makes that it possible to forecast the performance of PV systems in the three climate zones. In all three zones throughout this time, a consistent temperature pattern was seen. Zone 1 has a high annual average temperature, which falls from zone 1 to zone 3 as the year progresses. Given that the Sahelian strip has daily temperatures that can exceed 40°C, zone 3 should theoretically perform better for PV systems than zone 2 because of this and zone 2 will perform better than zone 1. According to Ouedraogo et al. [6], temperature can impair the performance of silicon photovoltaic cells. The monthly average temperature evolution in the figure 8 from 2015 to 2020 is evaluated using Ouagadougou, a city in zone 2, which is situated in the center of this country and at the same time in the center of West Africa.

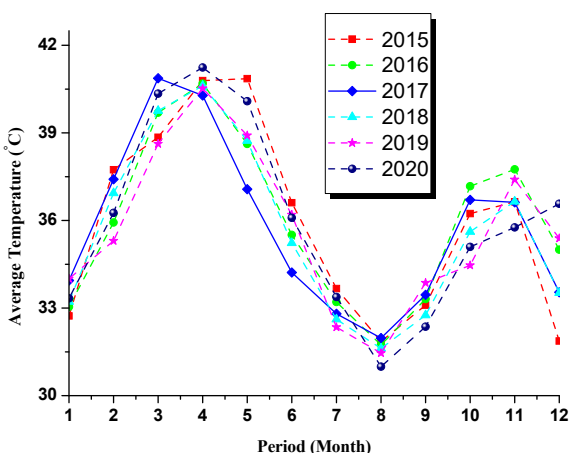


Figure 8: Seasonal cycle of air temperature in Ouagadougou from 2015 to 2020

The figure 8 shows three essential traits. April was the hottest month on average from March through May, except for 2015 and 2020. According to Kabore *et al.* [19], the average daily sunshine duration in these months ranges from 7 to more than 9 hours. It is then a best period for the PV energy production if the well PV modules are chosen taking into account the performances degradations versus the temperature. In a second hot spell that lasts from September through November, October is the hottest month. Additionally, PV energy is generated at a second, higher level. The last characteristic is freshness from December to February, with December being the coldest month. The drop in temperature was brought on by an increase in humidity and the rains in August. The temperature pattern found in Figure 8 is similar in the other climatic zones of the Sahel. According to Kabore *et al.*[19], the average daily sunshine duration in these months ranges from 7 to more than 9 hours. The Ouagadougou measurements of the sun global irradiation are displayed in figure 9.

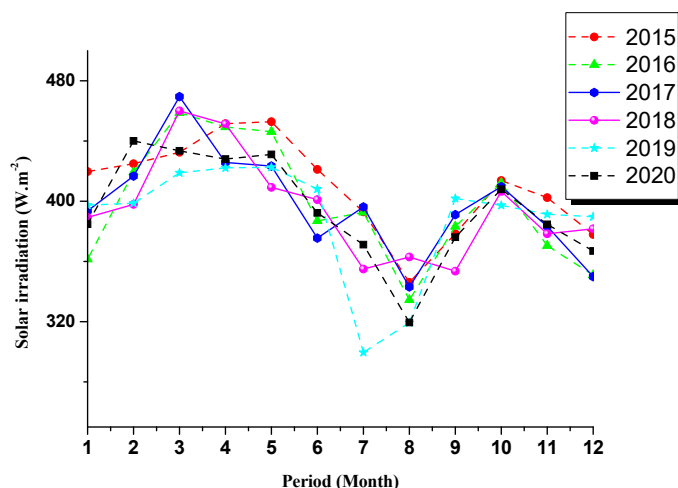


Figure 9: Average monthly global irradiation over Ouagadougou

The best solar global irradiation is obtained in the period from March to May. Using the equation (2), theoretically the best PV energy production will be found in this period. The second best solar global irradiation period is between September to November. It is so the second best PV energy production period. Following the observations from the figure 8, theoretically the best energy production will be the month of April followed by the month of October in the year. The month of August will be the worst month of the PV energy production because of the humidity due to the rainfall. During the months of March through May, the best global irradiance is attained. The optimal time for PV energy generation will be discovered in this time frame, according to the equation (2). September through November has the second-best solar irradiance levels. The best energy production will, in theory, occur in the months of April and October of a given year, as shown by the observations from the figures 8-9. Because of the humidity from the rains, August will be the worst month for producing PV electricity.

3.2. In-situ Production of PV Energy in the Climatic Zones

Figure 10 presents the PV energy produced in the three climatic zones of Burkina Faso.

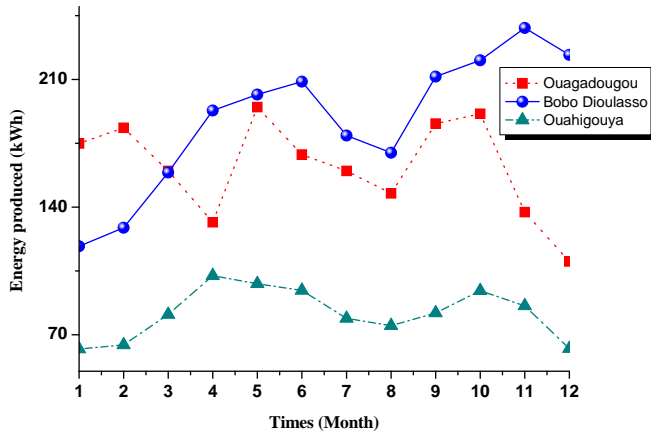


Figure 10: Average production of monthly PV energy in the three climatic zones of Burkina Faso

In all three climate zones, the same power peak $50kW_p$ is generated. Bobo Dioulasso (zone 3) and Ouagadougou (zone 2) have higher connected loads than Ouahigouya (zone 1). Compared to Bobo Dioulasso and Ouagadougou, Ouahigouya has a higher average temperature. The observations in the figures 8, 9 and 10 are consistent with one another. Compared to zones 2 and 3, the level of dust in zone 1 is particularly significant. The short production time of eleven days, not thirty-one days, is what accounts for the high production seen in the first month in zone 2. In zone 1, the months of April and October have the best PV production. In zone 2, the best PV production occurs between May and October. The best months for solar energy production in zone 3 are June and November. There is consistency between the installed PV system production and the theoretical predictions in the various scenarios, as shown by some research [11, 20, 10]. However, because to the national grid's frequent power shortage, April is the poorest production month in zone 2 overall. The national grid receives a significant demand due to the hot period, which results in the battery bank replacing the national grid to assure the continued injection of solar energy. According to estimates, the national grid is unavailable for 177 hours, or 2%, on average, per year. However, according to SONABEL [21], the rural areas are above this average. This means that for the three climate zones, it is projected that the failure rate of the PV power plant will be close to zero percent. The battery bank does really take over when the SONABEL is unavailable. The produced energy on the reference figure 10 is greater than what the load in zone 1 consumes. The University of Ouahigouya shuts down every day at 4:00 pm (GMT) due to the security issues in this region. What makes it difficult to understand the necessity for batteries. That is not the case with the remaining two zones, which are shown in the figure 11. This graph shows that both sections of the battery system are

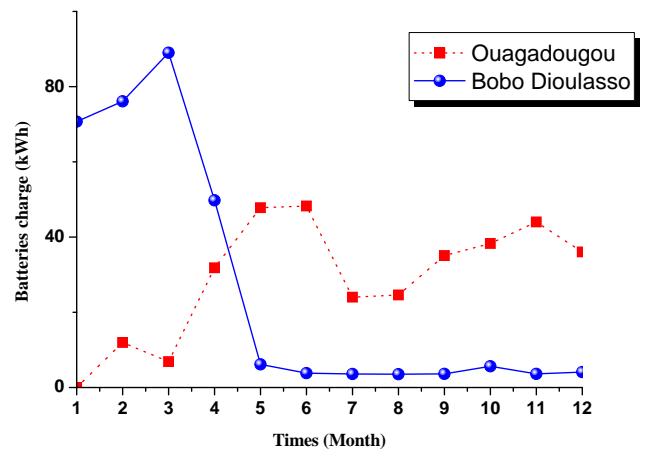


Figure 11: Batteries charge in two climate zones

correctly charged. The incorrect PV system arrangement, however, is consistent with the excessive charge seen in the Bobo Dioulasso. PV energy, batteries, and the national grid are used in that order, from beginning to end, for energy consumption. That explains the increased battery usage from January to March shown in figure 12. This arrangement was changed from May to December to one that was based on the placement of the batteries, the national grid, and PV energy. This enables the battery usage to decrease and thus lengthen the battery life. For the same capacity in a good configuration, Ouagadougou's charge is more significant than Bobo Dioulasso's. In contrast to a university in zone 3 of Bobo Dioulasso, the PV system is built in a hospital in zone 2 of Ouagadougou where nocturnal activities are quite essential. Figure 12 shows that many storage batteries are used.

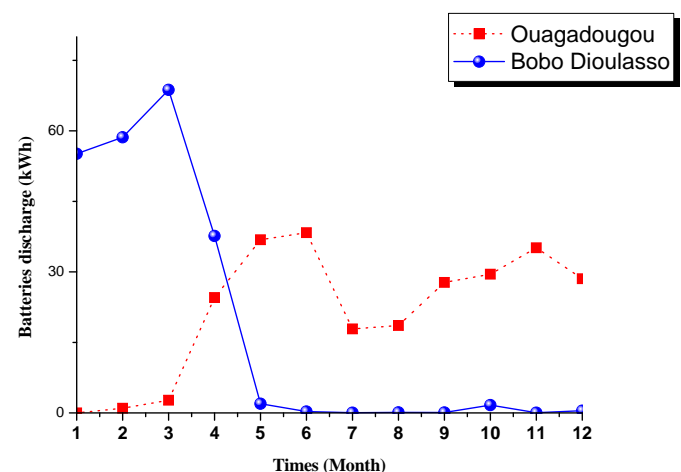


Figure 12: Batteries discharge in two climate zones

The configuration issue can be seen in these curves as well. Compared to the Nazi Boni University of Bobo Dioulasso, the

Ouagadougou hospital has a stronger battery discharge in the ideal configuration from May to December. Because of the increased demand on the national grid brought on by the heat wave, which frequently results in grid outages, the need of batteries for the hospital PV system is highlighted from April to July. From September through December, a second emphasis on battery use is seen. The Sahelian strip's PV energy output improved for the second time in the year during this study period. The significant energy demand on the batteries, however, can be explained by the dust and the little sunshine in December.

4. Conclusion

March through May, with April being the hottest month outside of 2015 and 2020. Sunlight exposure ranges from 7 to more than 9 hours every day. That explains, both theoretically and experimentally, the strong PV energy output in this month's range. The PV module's efficiency, however, is adversely impacted by the high temperature. The warmest month of the second heat wave is October, which lasts from September to November. The PV energy generation is likewise good in this second range. The primary environmental factor affecting PV module efficiency is temperature. There is a set battery charge and discharge. The arrangement of direct PV energy, the national grid, and the batteries at the end is suitable for PV installations in various temperature zones. For the three climate zones, the anticipated failure rate of the PV power plant is close to 0%. The batteries do indeed take over when the SONABEL is not available. The Sahelian climate zone records its best PV energy output in April, followed by its second-best PV energy production in October. The Sudano-Sahelian climate produces the most solar energy between the months of May and October. June and November are the ideal times of year to produce solar energy in the Sudanese environment. The actual energy output of the PV system, the theoretical predictions, and the literature research are all consistent in the various scenarios. The present study shows the security in the Sahel weakens the PV energy deployment. The load estimation is an important factor to succeed the installation and the optimum operation of the PV power plant.

References

- [1] Diego Martinez-Plaza, Amir Abdallah, Benjamin W. Figgis, and Talha Mirza. Performance improvement techniques for photovoltaic systems in qatar : Results of first year of outdoor exposure. *Energy Procedia*, 77:386–396, 2015. 5th International Conference on Silicon Photovoltaics, SiliconPV 2015.
- [2] Ali Omar Mohamed and Abdulazez Hasan. Effect of dust accumulation on performance of photovoltaic solar modules in sahara environment. *Journal of Basic and Applied Scientific Research*, 2(11):11030–11036, 2012.
- [3] Direction gnrale des tudes et des statistiques sectorielles (DGESE). Annuaire statistique 2018 du ministre de lnergie. techreport, Ministre de lnergie, www.energie.bf, December 2019.
- [4] Kokouvi Edem N'tsoukpoe, Blandine Bambara, and Madieumbe Gaye. Rapport de l tude de marche solaire thermique: production d'eau chaude et de schage des produits agricole au Burkina Faso. Technical report, Centre pour les nergies Renouvelables et l'Efficacit Energtique de la CEDEAO (ECREEE), December 2015.
- [5] Adama Ouedraogo, Amadou Diallo, Soumala Goro, Wend Dolean Arsene Ilboudo, Sadou Madougou, Dieudonn Joseph Bathiebo, and Si Kam. Analysis of the solar power plant efficiency installed in the premises of a hospital Case of the Pediatric Charles De Gaulle of Ouagadougou. *Solar Energy*, 241(2022):120–129, June 2022.
- [6] Adama Oudraogo, Bernard Zouma, Emmanuel Oudraogo, Lamoussa Guissou, and Dieudonn Joseph Bathibo. Individual efficiencies of a polycrystalline silicon PV cell versus temperature. *Results in Optics*, 4, 08 2021.
- [7] D. T. Cotfas, P. A. Cotfas, and O. M. Machidon. Impact of temperature on performance of series and parallel connected mono-crystalline silicon solar cells study of temperature coefficients for parameters of photovoltaic cells. *International Journal of Photoenergy*, 2018, 2018.
- [8] Ouedraogo Adama, Boubacar Soro, Konate Ramatou, Oumarou Fati Amadou, and Bathiebo Dieudonn Joseph. Investigation of the polycrystalline silicon PV cell efficiency in 3D approximation versus electromagnetic field under monochromatic illumination. *International Journal of Photoenergy*, 2021, 2021.
- [9] Ouedraogo Adama, Savadogo Mahamadi, Honadia Prince Abdoul Aziz, Bathiebo Dieudonne Joseph, and Kam Sie. Individual energetic processes efficiencies in a polycrystalline silicon PV cell versus electromagnetic field. *Silicon*, 2021.
- [10] Abdoulatif Bonkaney, Saïdou Madougou, and Rabani Adamou. Impacts of cloud cover and dust on the performance of photovoltaic module in niamey. *Journal of Renewable Energy*, 2017.
- [11] A. Ouedraogo, H. Guengane, K. Imbga, and D. J. Bathiebo. Analysis of external load resistance influence on the single-crystalline silicon photovoltaic module (PV). *Journal of Fundamental and Applied Sciences*, 11(2):663–674, May 2019.
- [12] A.S.O. Ogunjuyigbe, T.R. Ayodele, and O.A. Akinola. Optimal allocation and sizing of PV/wind/split-diesel/battery hybridenergy system for minimizing life cycle cost, carbon emission and dumpenergy of remote residential building. *Applied Energy*, 171:153–171, 2016.

- [13] Bukara Abba Lawan, Tana Chee Wei, and Lau Kwan Yiew. Optimal sizing of an autonomous photovoltaic/wind/battery/dieselgenerator micro-grid using grasshopper optimization algorithm. *Solar Energy*, 188:685 – 696, 2019.
- [14] Liu Hao, Wu Baojia, Maleki Akbar, Pourfayaz Fathollah, and Ghasempour Roghayeh. Effects of reliability index on optimal configuration of hybridsolar/battery energy system by optimization approach : Acase study. *International Journal of Photoenergy*, 2021, 2021.
- [15] Huan-Liang Tsai. Insolation-oriented model of photovoltaic module usingmatlab/simulink. *Solar Energy*, 84:1318 – 1326, 2010.
- [16] Ayop Razman and Tan Chee Wei. A comprehensive review on photovoltaic emulator. *Renewable and Sustainable Energy Reviews*, 80:430 – 452, 2017.
- [17] Jean Menendi. Dimensionnement d'un gnrateur photovoltaïque, informatisation du procede. Master's thesis, E.I.E.R, 1990.
- [18] Waongo M., Koalaga Z., and Zougmore F. A guideline for sizing photovoltaic panels across different climatic zones in burkina faso. *IOP Conf. Series: Materials Science and Engineering*, 29:012 – 014, 2012. 1st International Symposium on Electrical Arc and Thermal Plasmas in Africa (ISAPA).
- [19] Boureïma Kabore, Kam Si, Ouedraogo Germain Wende Pouire, and Bathiebo Dieudonne Joseph. Etude de l'volution climatique au burkina faso de 1983 2012 : cas des villes de Bobo Dioulasso, Ouagadougou et Dori. *Arabian Journal of Earth Sciences*, 4(2):50 – 59, 2017.
- [20] Ouedraogo Adama, Mogmenga Ladifata, Bado Nébon, Ky Thierry Sikoudouin Maurice, and Bathiebo Dieudonné Joseph. Analysis of the single-crystalline silicon photovoltaic (pv) module performances under low γ - radiation from radioactive source. *Silicon*, 12:18311837, 2020.
- [21] SONABEL. Rapport d'activits 2020. Technical report, 2021.